

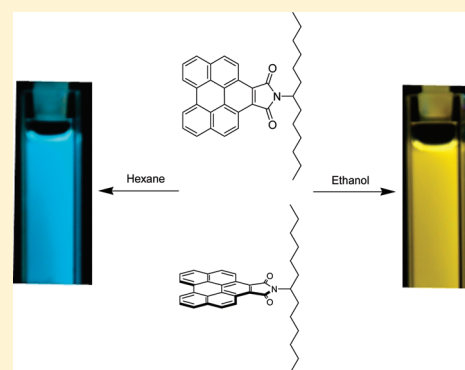
Synthesis, Characterization, and Photophysical Study of Fluorescent N-substituted Benzo[ghi]perylene “Swallow Tail” Monoimides

Steven J. Manning, William Bogen, and Lisa A. Kelly*

Department of Chemistry and Biochemistry, University of Maryland, Baltimore County, 1000 Hilltop Circle, Baltimore, Maryland 21250, United States

S Supporting Information

ABSTRACT: A set of N-substituted benzoperylene monoimide (BPI) fluorophores was synthesized and characterized structurally and photophysically. Condensation of benzo[ghi]perylene-1,2-dicarboxylic anhydride in the presence of “swallow tail” alkyl amines produced fluorophores that are soluble in a range of organic solvents, highly absorbing in the near-UV ($\epsilon_{334} = 79\,000\text{ M}^{-1}\text{ cm}^{-1}$), and fluorescent in the visible range. Photophysical behavior of the compounds was studied with steady-state and time-correlated single photon counting. The synthesized BPIs exhibit positive solvachromatic emission ($\lambda_{\text{em}}(\text{hexane}) = 469\text{ nm}$; $\lambda_{\text{em}}(\text{ethanol}) = 550\text{ nm}$) as a function of solvent polarity with little change in their excited-state lifetime (9.6–6.5 ns) and fluorescence quantum yield (0.27–0.44) over the polarity range studied. Solvachromatic shifts were analyzed using the Lippert–Mataga approach. In nonpolar hydrocarbon solvents evidence of dual emission from closely spaced (562 cm^{-1}) S_1 and S_2 excited states is observed. Preliminary peak assignments for the anomalous S_2 emission are made.



INTRODUCTION

Molecular fluorophores are valuable tools as reporters of local environment in many biological and macromolecular systems. Highly conjugated polyaromatic derivatives of perylene and benzoperylene have received considerable research interest as vat dyes and versatile molecular fluorophores.^{1–3} These compounds exhibit many qualities advantageous to the optical sensing and information recording fields including high quantum yields,^{4,5} photostability,⁶ and inertness to aggressive chemical reagents. Their application in light harvesting,^{7,8} as laser dyes,^{9–14} and supermolecular architectures^{15–22} has been promising and well-documented. In addition, dyes that exhibit these features coupled with solvachromatic emission have the potential to detect polarity changes in complex environments.

Benzo[ghi]perylene monoimides (BPIs) represent a unique class of fluorescent perylene dyes. Three variations of BPI derivatives have been documented; however, their photophysics have not been thoroughly examined.^{23–25} Specifically, solvent-dependent absorption and emission properties have not been previously reported. While their structures suggest that they retain the chemical and photophysical stability of their widely studied perylene bisimide and diimide counterparts, we show that BPIs exhibit strongly positive solvachromatic emission as a function of solvent polarity, with negligible changes in the near-UV range absorption maxima. With little hydrogen bonding and acid–base character, the solvachromatic shifts observed with changes in solvent polarity are likely general in nature.

Functionalization of the fluorophores at the imide nitrogen with ditert-butyl or “swallow tail” alkyl chains has some distinct advantages. First, the solubility of the dye is greatly increased in a range of common organic solvents. Moreover, the perpendicular geometry of the swallow tail with respect to the rigid aromatic ring system prevents aggregation from planar stacking.^{26,27} Most importantly, modifications with alkyl chains do not affect the electronic structure of the ring system; thus, their photophysical properties are not altered.

Solvachromatic dyes are those which exhibit shifts in their electronic spectra as a function of solvent interactions.²⁸ Although broad in scope, the influence of solvents on the excited-state chemistry of fluorophores can be divided into two types of effects; general and specific solvent effects. General solvent effects include the change in energy observed in absorption or emission resulting from the polarizabilities of the fluorophores and solvent, respectively. These interactions are, as their name implies, general in nature and include solvent dielectric (ϵ) and refractive index (n) terms. Specific solvent effects pertain to hydrogen bonding, acid base chemistry, or other particular solvent-fluorophore interactions that alter the excited-state chemistry. Fluorophores that do not exhibit substantial specific solvent effects can therefore be used as reliable indicators of local environment, such as solvent polarity. In this work, we present the synthesis and characterization of a set of “swallow tail” N-substituted benzo[ghi]perylene-1,2-dicarboxylic monoimides

Received: March 9, 2011

Published: June 07, 2011

Scheme 1. Synthesis of BPIs

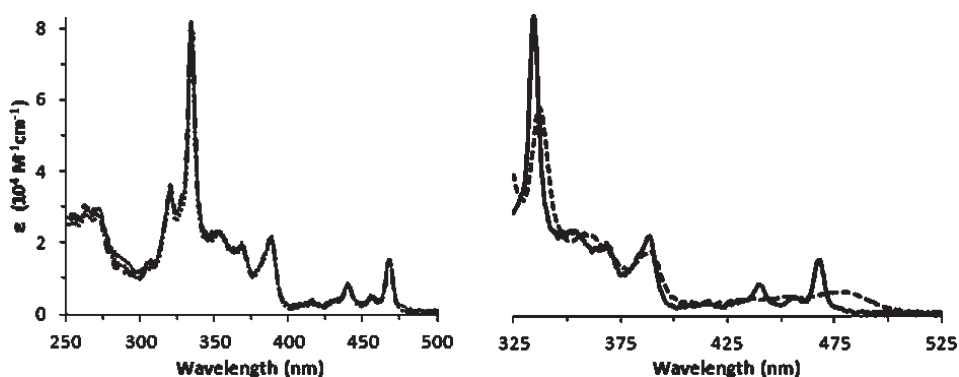
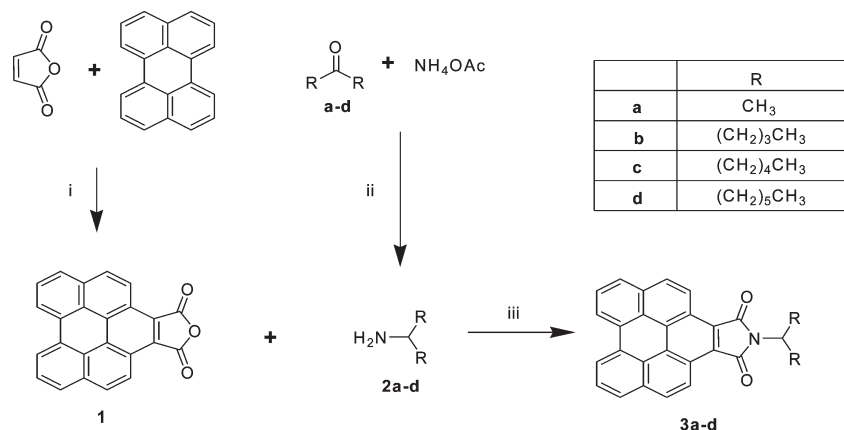


Figure 1. (Left) UV-vis absorption spectra of 3b (dash), 3c (dot), and 3d (solid) in hexane. (Right) Absorption spectra of 3d in hexane (solid) and ethanol (dash).

via a two step process. Also, their absorption and solvachromatic emission behavior are introduced. We analyze their solvachromatic behavior with the Lippert–Mataga approach and provide evidence of anomalous $S_2 \rightarrow S_0$ emission in nonpolar hydrocarbon solvents. Together, their simple synthesis, ease of purification, and photophysical properties suggest they have great utility in “smart” packaging and optical sensing fields.

RESULTS

Synthesis of Benzoperylene Monoimides. The synthesis of benzoperylene monoimides 3a–d was completed via condensation of “swallow tail” amines 2a–d in the presence of 1 as illustrated in Scheme 1. The inclusion of a bulky alkyl chain “swallow tail” at the imide nitrogen has been shown to greatly improve solubility of similar fluorophores by sterically hindering aggregation.^{3,26} Step (i) shows the formation of 1 via the well-documented Diels–Alder reaction of perylene and maleic anhydride in the presence of the strongly oxidizing agent p-chloranil, as developed by Clar.^{29–31} This reaction was chosen as it exhibits quantitative yields and short reaction times. Product 1 is readily crystallized and serves as the precursor for the synthesis of the new monoimide fluorophores. Target compounds 3a–d were isolated via reductive amination of ketones a–d (step (ii)) with sodium cyanoborohydride according to the Borch amine synthesis.³² The condensation step (iii) was devised by our group according

Table 1. Photophysical Data for 3d in Solvents of Increasing Polarity

solvent	ϵ (25 °C)	λ_{\max} (nm) ^a	ϵ_{\max} (M ⁻¹ km ⁻¹) ^b	λ_{em} (nm) ^{a,e}	τ (ns) ^{c,e}	Φ_{f} ^{d,e,f}
hexane	1.882	334	79000 (±1900)	469	9.5	0.32
cyclohexane	2.015	335	73700 (±1200)	471	10.5	0.32
CCl ₄	2.228	338	56600 (±3400)	482	8.7	0.37
toluene	2.379	339	50200 (±900)	491	9.2	0.42
ethyl ether	4.329	335	54600 (±1600)	495	9.6	0.34
acetone	20.70	336	51600 (±1900)	514	7.8	0.27
chloroform	4.806	339	60100 (±900)	522	6.7	0.35
acetonitrile	37.50	336	51900 (±800)	527	7.5	0.33
DMSO	46.70	339	52000 (±1200)	534	7.7	0.44
ethanol	24.30	336	55200 (±1800)	550	6.5	0.30

^a ±1 nm. ^b $r^2 > 0.996$. ^c ±0.1 ns. ^d ±0.05. ^e Emission data obtained at λ_{\max} for each solvent. ^f Quantum yields measured using quinine sulfate in 0.1 M H₂SO₄.

to similar syntheses of perylene-3,4,9,10-tetracarboxylic bisimide dyes.^{4–6,25,33}

BPIs 3b–d were produced in high yields. These yields decreased from 89% to 76% for 3b to 3d, respectively. However, the yield of compound 3a was significantly lower. Product solubility and melting point ranges also show trends with increasing

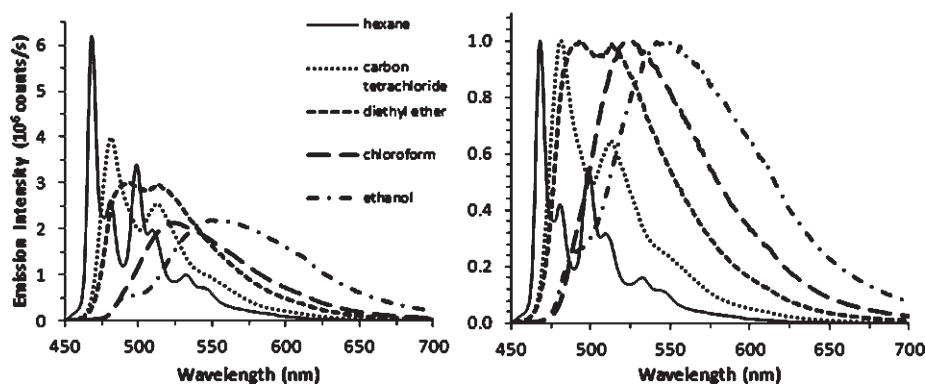


Figure 2. (left) Fluorescence spectra of $12 \mu\text{M}$ **3d** in solvents of increasing polarity. (right) Normalized fluorescence emission of **3d**. Spectra recorded at 22°C . An excitation wavelength of 336 nm was used.

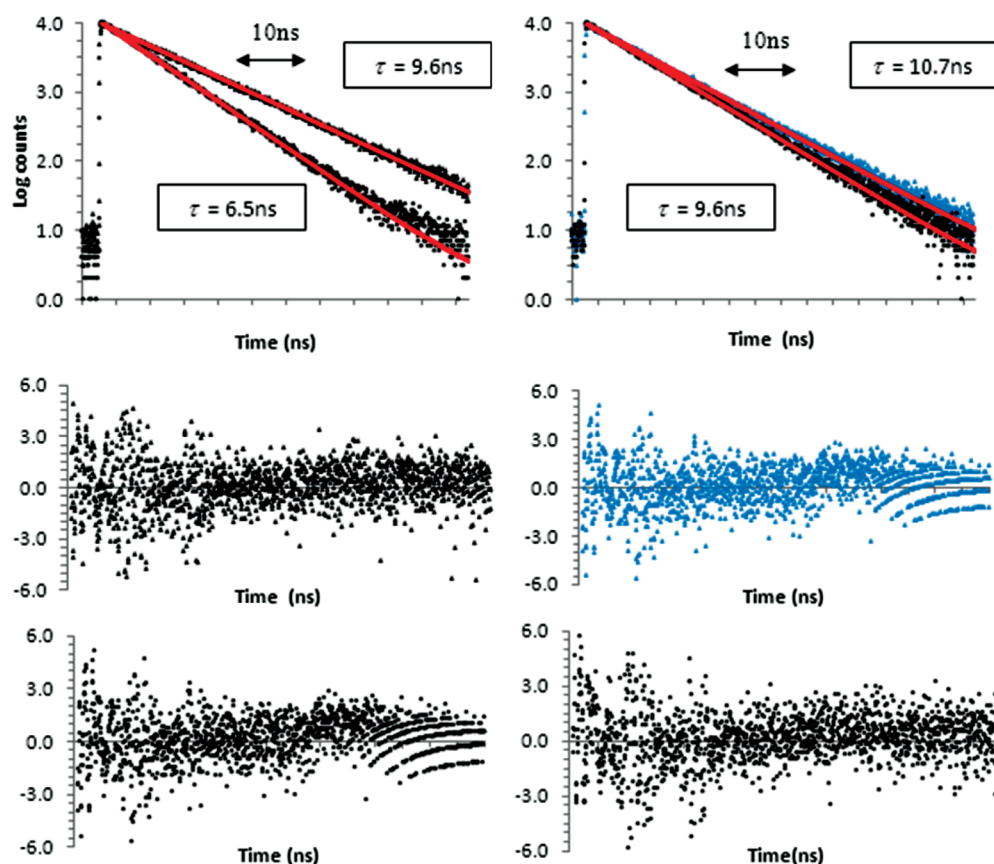


Figure 3. Time correlated single photon counting decay traces of (top left) $90 \mu\text{M}$ **3d** in hexane; $\lambda_{\text{em}} = 468 \text{ nm}$ (triangles) and ethanol, $\lambda_{\text{em}} = 550 \text{ nm}$ (diamonds), (middle left/bottom left). Weighted residuals plot of decay fit for **3d** in hexane and ethanol. (top right) $90 \mu\text{M}$ **3d** in hexane emission at 456 nm (blue) and 468 nm (black), (middle right bottom right). Weighted residuals of **3d** in hexane with emission at $456 \text{ nm}/468 \text{ nm}$. All spectra at 22°C . An excitation wavelength of 394 nm was used.

“swallow tail” chain length. The solubility of the products increased with longer tail length, with **3a** having very low solubility in organic solvents, so low in fact that it approaches the insolubility of compound **1**. The melting points of **3a–d** show a systematic decrease from $>320^\circ\text{C}$ to 187°C as a function of alkyl side chain length. The low solubility of **3a** limits the ability to fully characterize the compound. Therefore, only **3b–3d** were spectroscopically examined.

The new compounds were characterized using ^1H and ^{13}C NMR, FTIR, elemental analysis, and mass spectrometry. Previously

prepared perylene imide dyes maintain a perpendicular geometry of the imide nitrogen substituent with respect to the aromatic ring system.^{3,21,27,34,35} This orientation is found in the new BPIs and supported by the observation of two separate methylene signals at 1.85 and 2.25 ppm in the ^1H NMR spectra. It is likely that this behavior is the result of the nonequivalent interaction between the two methylene groups of the alkyl tail with the carboxamide oxygens. Changes in the imide alkyl chain length are confirmed in the different integration values of the ^1H NMR signals appearing at $1.30\text{--}1.45 \text{ ppm}$ while the aromatic and

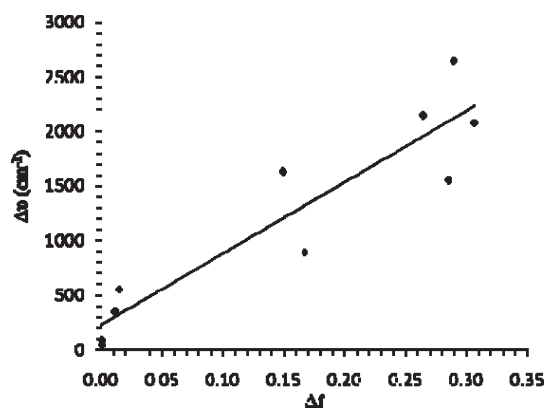


Figure 4. Lippert–Mataga plot of the $S_1 \rightarrow S_0$ Stokes' shift observed for **3d** in solvents of increasing polarity.

methine (^1H at 4.4 ppm) signals remain unchanged. Upon addition of an alkyl “swallow tail”, some other changes are observed that are useful for product characterization. FTIR spectra reveal the appearance of new C–H stretches between 2850 and 2960 cm^{-1} and a peak at 1692 cm^{-1} , indicating the formation of the disubstituted carboxylic imide, all of which are absent in the starting compound **1**. Differences in the swallow tail length can be monitored by the peak integrations in the 10–30 ppm region of the ^{13}C NMR spectra.

Absorption Properties. The UV–vis absorption spectra of the BPIs **3b–d** in hexane, as well as **3d** in hexane and ethanol, are shown in Figure 1. The compounds exhibit the same absorbance features independent of “swallow tail” chain length. In hexane, each compound shows structured transitions with peaks at 468, 456, 440, 432(shoulder), and 416 nm in the visible region and 389, 369, 355, 334(max), and 320 nm in the UV. The lowest energy transition is attributed to the $S_0 \rightarrow S_1$ transition at 468 nm with a molar absorptivity (ϵ) of 15 200 $\text{M}^{-1}\text{cm}^{-1}$, far lower than the visible range absorbance of its perylene bisimide counterparts ($\epsilon > 90\,000\ \text{M}^{-1}\text{cm}^{-1}$).¹⁸ The strongest absorbance peak of the BPIs is the $\pi \rightarrow \pi^*$ transition at 334 nm with a molar absorptivity of 79 000 $\text{M}^{-1}\text{cm}^{-1}$. The absorption peak energies and shapes are consistent with other structurally similar fluorophores.^{29,36} Hypsochromic and bathochromic shifts, as well as band broadening, are observed for the absorbance peaks of the BPIs in more polar solvents. Some of these trends are outlined in Table 1 for a range of 10 solvents. The band broadening and red-shift is more pronounced in the low energy visible range of the spectra. For example, in ethanol the absorbance maxima red-shifts 3 nm in the UV, while an 11-nm red-shift is observed for the $S_0 \rightarrow S_1$ peak with respect to hexane spectra. The full width half-maximum of the low energy transition increases from 6 to 40 nm in hexane and ethanol, respectively. This band broadening suggests there is a decrease in the vibrational spacing of the excited state surface. A possible explanation for this is the existence of a mixed $n \rightarrow \pi^*$ and $\pi \rightarrow \pi^*$ excited state. This is supported by the molar absorptivity of the transition (15 200 $\text{M}^{-1}\text{cm}^{-1}$) as it is between the accepted values for the two independent types of transitions.³⁷

Fluorescence Properties. The excited-state properties of BPIs were investigated using fluorescence emission spectroscopy. The emission spectra of **3d** in solvents of increasing polarity are shown in Figure 2 and summarized in Table 1. In hexane and other alkyl chain hydrocarbon solvents, the BPIs exhibit structured absorbance and emission in the visible range. Alternating

Table 2. Calculated Dipole Moment Changes and Excited States Dipole Moments of **3d**

n (Å)	$\Delta\mu$ (D)	μ_o (D) ^a
3.0	4.2	7.7
3.5	5.3	8.8
4.0	6.5	10.0
4.5	7.7	11.2

^a Calculated via AMI method.

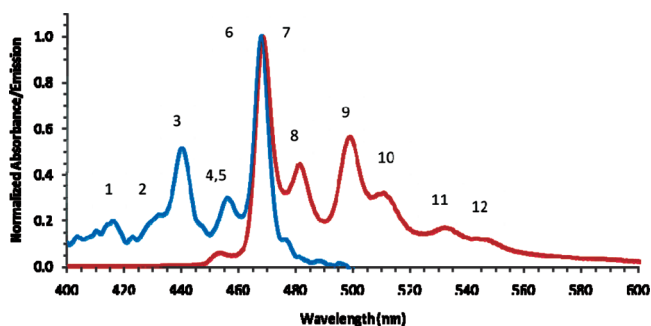


Figure 5. Combined absorption and emission spectra of **3d** in hexane at 22 °C. Peak numbers correspond to assignments in Table 3.

band intensity and a mirror image relationship is observed with substantial overlap of the most intense band at 469 nm. As the solvent polarity increases, a Stokes' shift was observed and the mirror image relationship lost. Over the polarity range of hexane to ethanol, the emission maxima increased from 469 to 550 nm, respectively. Again, band broadening is observed as a function of solvent polarity and the vibrational structure disappeared in solvents more polar than diethyl ether. Fluorescence quantum yields (Φ_f) were determined to be between 0.27 and 0.44 over the range of solvents studied. Time correlated single photon counting decay traces of **3d** are shown in Figure 3. The excited-state lifetime (τ) of **3d** decays as a single exponential in all solvents and decreases with solvent polarity from 9.6 to 6.5 ns in hexane and ethanol, respectively. The excited state lifetime of **3d** in hexane maintains a single exponential decay at all emission wavelengths, but the value of the lifetime is longer (10.7 ns) for emission at 456 nm than at all other emission wavelengths (9.6 ns). A statistical analysis of the fits was performed, yielding relative errors of 0.6% for each within a 95% confidence interval. This suggests that the lifetimes are indeed statistically different at the respective emission wavelengths.

In hexane and other hydrocarbon solvents, unique emission behavior is observed. As mentioned above, under these conditions, there is a clear mirror image relationship between absorbance and emission. However, the spacing between adjacent bands follows an alternating pattern indicative of emission from multiple excited states. These findings and their peak assignments are presented in subsequent sections.

DISCUSSION

Synthesis and Chemical Properties of BPIs. The observed decrease in product yield with longer “swallow tails” is to be expected from the increased steric bulk of the 13-carbon tail added and the deviation from the structure of starting material **1**. These trends in solubility and melting point are the result of

Table 3. Peak Assignments of Electronic Transitions of 3d in Hexane

peak	type	$\nu' \rightarrow \nu''$	λ (nm)	ΔE (cm ⁻¹)	peak	type	$\nu' \rightarrow \nu''$	λ (nm)	ΔE (cm ⁻¹)
1	S ₀ → S ₁	0,2	416.0	24038	2	S ₀ → S ₂	0.1	432.0	23143
3		0,1	440.0	22727	4		0.0	456.0	21930
6		0,0	458.0	21368	5	S ₂ → S ₀	^a	^a	^a
7	S ₁ → S ₀	0,0	459.5	21299	8		0.1	482.5	20725
9		0,1	500.0	20000	10		0.2	510.5	19589
11		0,2	533.0	18762	12		0.3	544.0	18382

^a Peak position distorted due to strong self-absorption.

disrupted planar stacking of the molecules by the longer bulky alkyl chains. They agree with those observed for similar “swallow tail” perylene diimides in previous reports.³⁸

Photophysics and Solvatochromism. The synthesized BPIs exhibit positive solvachromatic emission as a function of solvent polarity, a phenomena well documented in the literature.^{28,39} Analysis of the solvachromatic shifts using the Lippert–Mataga approach employs eqs 1 and 2, where $\Delta\nu$ is the observed Stokes' shift of the lowest energy electronic transition (in cm⁻¹), Δf is the solvent polarizability parameter, a is the Onsager cavity radius of the dipole, μ_e and μ_g are the dipoles of the excited and ground states, and h and c are Planck's constant and the speed of light, respectively. In eq 2, ϵ and n are the solvent dielectric constant and refractive index values, respectively.³⁹

$$\Delta\nu = \frac{2\Delta f}{hca^3} (\mu_e - \mu_g)^2 + C \quad (1)$$

$$\Delta f = \frac{\epsilon - 1}{2\epsilon + 1} - \frac{n^2 - 1}{2n^2 + 1} \quad (2)$$

A plot of Δf vs $\Delta\nu$ as observed from the absorbance and emission spectra of 3d in solvents of increasing polarity is shown in Figure 4. A linear least-squares fit to eq 1 yields a slope of 6540 cm⁻¹ with an r^2 of 0.86. With knowledge of μ_g (3.5 D) and a , μ_e can be obtained. Due to the contention on the issue of Onsager radii size, Table 2 presents the calculated $\Delta\mu$ values determined via the AM1 computational method with three estimations of the cavity radius between 3.0 and 4.5 Å. The positive slope of the Lippert–Mataga plot in the solvents studied suggests that general solvent effects are responsible for the observed positive solvatochromic shifts in emission. Due to the fact that the ground state dipole moments are significantly smaller than those in the excited state, strong solvatochromism is observed in emission, but only weakly in absorption. However, its low correlation coefficient of 0.86 supports the influence of some specific solvent effects. Most notably, halogenated solvents seem to increase the red-shift observed in emission and shorten the excited state lifetime. A more thorough investigation of the nature of these specific solvent effects is currently underway to ascertain the influence of hydrogen bonding and halogenations of solvents.

Anomalous S₂ Fluorescence. In nonpolar hydrocarbon solvents, the BPIs display unique electronic behavior indicative of two closely spaced emissive singlet states, S₁ and S₂. The peak assignments in Figure 5 and Table 3 are representative of this two-state model. According to Kasha's Rule,⁴⁰ the fluorescence of a molecule in condensed media occurs only from the lowest vibrational level of the lowest electronic excited state, S₁, since vibrational relaxation proceeds much faster (picoseconds) than the time scale of fluorescence (nanoseconds). Although this rule is well-accepted, some exceptions do exist, most notably the S₂ → S₀

fluorescence of azulene.^{41,42} Also, 1,12-benzoperylene and other bay-substituted perylene derivatives have shown evidence of dual S₂ and S₁ emission at room temperature in previous studies.^{43–47} For the most structurally similar fluorophore that exhibits this dual emission behavior (1,12-benzoperylene), two excited singlet states S₁ (¹L_b) and S₂ (¹L_a) are assigned to be separated by less than 1400 cm⁻¹.⁴⁷ At 23 °C, significant thermal population of S₁ → S₂ occurs, and dual emission is observed.

In the case of BPIs 3b–c, spectra indicate that there is even closer spacing of the S₁ and S₂ levels than that observed in the previously studied compounds, and that their lowest vibrational states separated by only 562 cm⁻¹. The Boltzmann populations of the two states can be calculated using eq 3 where N_S are the populations of the S₂ and S₁ states, E is the energy of the states, k_B is the Boltzmann constant, and T is the absolute temperature.

$$\ln\left(\frac{N_{S_2}}{N_{S_1}}\right) = \frac{-(E_{S_2} - E_{S_1})}{k_B T} \quad (3)$$

With such small spacing between the S₁ and S₂ excited states, 6.4% of the molecules are expected to be able to populate the S₂ state at room temperature. Excited-state lifetime measurements of the samples produced single exponential decays at emission peaks 5 and 7–12, with peaks 7–12 yielding identical lifetimes of 9.6 ns. Only peak 5 produced a different lifetime of 10.7 ns. The longer lifetime emission at peak 5 is consistent with emission from the thermally populated S₂ → S₀ state, as it occurs slightly delayed from that of S₁. Further low temperature fluorescence experiments are underway to better characterize the dual emission.

CONCLUSIONS

In summary, we present the synthesis and characterization of a set of benzo[ghi]perylene N-substituted monoimide fluorophores were prepared via condensation of benzo[ghi]perylene-1,2-dicarboxylic anhydride and various “swallow tail” alkyl chain amines. The products are soluble in a range of organic solvents and show positive solvachromatic emission as a function of solvent polarity. They maintain the properties desirable for industrial molecular fluorophores including synthetic ease, high chemical and photochemical stability, and moderately high fluorescence quantum yields ($\Phi_f > 0.27$) in all solvents examined. Also, they strongly absorb in the near UV range, with much weaker absorbance in the visible range. This property, coupled with their solvachromatic emission, suggests that they will be valuable tools as molecular reporters of local polarity in complex macromolecular systems including polymer matrices and nanoparticles. As expected, the photophysical properties do not change as a function of the length of the “swallow tail” chains.

In hydrocarbon solvents, the BPI fluorophores exhibit spectral characteristics of two closely spaced excited states (S_1 and S_2), separated by only 562 cm^{-1} . The vibrational assignments are tabulated from the electronic spectra and their alternating nature suggest that a two-state system is operative. Further low temperature fluorescence experiments are being conducted to analyze the nature of the observed phenomena; the results will be presented in future work.

EXPERIMENTAL SECTION

Benzo[ghi]perylene-1,2-dicarboxylic Anhydride (1). A 5.090-g portion of perylene (20.17 mmol) was dissolved in 80.57 g melted maleic anhydride (0.82 mol) at 240°C in a 250 mL two neck round-bottom flask equipped with stir bar and condenser. The mixture was brought to a rolling boil and 11.20 g p-chloranil (recrystallized from acetone) (45.60 mmol) was added in small portions over 10 min. The reaction was allowed to reflux for 10 min, after which 100 mL of hot xylenes was added and the flask brought to room T . Then, the thick red precipitate was filtered off and washed with xylenes and ether ($3 \times 100\text{ mL}$ each). Red solids were collected (99%) and boiled in 2:1 ethyl acetate/chloroform for 16 h and filtered hot to afford 5.793 g clean, dry product. (85% recovered). mp $> 320^\circ\text{C}$ FT-IR: 1831 cm^{-1} (m), 1816 (m), 1785 (w), 1766 (s), 1757 (s), 1330 (w), 1293 (s), 1217 (w), 1181 (s).

1-Butylpentylamine (2b). Portions of 5-nonanone (5.01 g, 35.2 mmol) and ammonium acetate (27.76 g, 360.1 mmol) were stirred at room temperature under N_2 gas in methanol (150 mL) for 90 min. Sodium cyanoborohydride (1.56 g, 24.8 mmol) was added and the solution was stirred for 56 h. The reaction was quenched by adding concentrated HCl dropwise (7 mL) and concentrated on a rotary evaporator. The white solid was dispersed in water (500 mL) and adjusted to pH 10.5 with KOH. The solution was extracted with methylene chloride (400 mL). The pale yellow oil (4.32 g, 86%) was obtained by concentrating the CH_2Cl_2 fractions. $^1\text{H NMR}$ (400 MHz, CDCl_3): δ 2.56 (m, 1H), 1.36 (s, 2H), 1.09–1.31 (m, 12H), 0.79 (t, $J = 6.6\text{ Hz}$, 6H). $^{13}\text{C NMR}$ (400 MHz, CDCl_3) δ 13.8, 22.7, 28.2, 37.5, 50.9.

1-Pentylhexylamine (2c). Portions of 6-decanone (5.03 g, 29.5 mmol) and ammonium acetate (20.06 g, 260.2 mmol) were stirred at room temperature under N_2 gas in methanol (150 mL) for 90 min. NaCNBH_3 (1.12 g, 17.8 mmol) was added and the solution was stirred for 56 h. The reaction was quenched by adding concentrated HCl dropwise (4 mL) and concentrated on a rotary evaporator. The white solid was dispersed in water (500 mL) and adjusted to pH 10.5 with KOH. The solution was extracted with methylene chloride (200 mL, 100 mL, and 100 mL). The pale yellow oil (4.8556 g, 96%) was obtained by concentrating the CH_2Cl_2 fractions. $^1\text{H NMR}$ (400 MHz, CDCl_3): δ 2.48 (m, 1H), 1.00–1.24 (m, 18H), 0.70 (t, $J = 6.2\text{ Hz}$, 6H) $^{13}\text{C NMR}$ (400 MHz, CDCl_3) δ 13.7, 22.4, 25.6, 31.8, 38.0, 50.9.

1-Hexylheptylamine (2d). A 5.650-g portion of dihexyl ketone (28.50 mmol) and a 21.97-g portion ammonium acetate (0.2850 mol) were dissolved in 85 mL methanol under N_2 for 30 min. 25 mL MeOH and 1.250 g sodiumcyanoborohydride (19.90 mmol) added to initiate reduction. The reaction was allowed to continue at room temperature with vigorous stirring for 48 h. The mixture was quenched with 3 mL concentrated HCl added dropwise and concentrated via rotary evaporation. The white solid was taken up in 500 mL H_2O and brought to pH 10 with KOH pellets. The solution was extracted with 400 and 200 mL CHCl_3 . Organics collected, dried over NaSO_4 , and evaporated to afford 3.6019 g 1-hexylheptylamine as a light yellow oil. (63%) $^1\text{H NMR}$ (400 MHz, CDCl_3): δ 2.48 (m, 1H), 0.93–1.25 (m, 22H), 0.69 (t, $J = 6.6\text{ Hz}$, 6H). $^{13}\text{C NMR}$ (400 MHz, CDCl_3) δ 13.9, 22.6, 26.1, 29.4, 31.8, 38.2, 51.1.

2-Isopropyl-1H-perylene[1,12-efg]isoindole-1,3(2H)-dione (3a). A 1.02-g portion of (1) (2.95 mmol) was dissolved in a solution of isopropylamine (0.5 g, 2.95 mmol) and 150 mL DMA. The

solution was refluxed overnight at 175°C , and then allowed to reach room temperature. A 230-mL portion of methanol was added and the red precipitate collected. The solid was boiled out in 1:1 methanol/water and collected by filtration to afford a 0.86 g of product. Mp.: $>320^\circ\text{C}$ Due to very low solubility no NMR data could be collected. FT-IR: 2925 cm^{-1} (w), 2855 (w), 1752 (w), 1696 (s), 1353 (m), 1309 (w), 1189 (w), 1050 (m), 1027 (m), 826 (s). Anal.: $\text{C}_{27}\text{H}_{17}\text{NO}_2$ Calcd., C (83.70), H (4.42), N (3.62), O (8.26); Found, C (83.12), H (4.48), N (3.56), O (8.84).

2-(Nonan-5-yl)-1H-perylene[1,12-efg]isoindole-1,3(2H)-dione (3b). A 1.73-g portion, 5.00 mmol, of (1) was added to a solution of (2b) (1.33 g, 9.35 mmol) in DMA (100 mL) and refluxed overnight. The solution was allowed to cool to room temperature and methanol (230 mL) was added to complete the crystallization. The obtained solid was dissolved in hot 4:1 toluene/hexane and purified by column chromatography (silica, toluene/hexane, $R_f = 0.55$), and finally boiled out in 200 mL methanol, leaving (3b) as an orange powder (2.09 g, 89%). Mp.: $226\text{--}228^\circ\text{C}$ $^1\text{H NMR}$ (400 MHz, CDCl_3): δ 9.30 (d, $J = 9.2\text{ Hz}$, 2H), 9.09 (d, 7.8 Hz, 2H), 8.27 (d, 7.8 Hz, 2H), 8.24 (d, 8.6 Hz, 2H), 8.13 (t, 7.8 Hz, 2H), 4.40 (sept, 4.8 Hz, 1H), 2.21–2.31 (m, 2H), 1.81–1.91 (m, 2H), 1.33–1.44 (m, 8H), 0.87 (t, 7.3 Hz, 6H) $^{13}\text{C NMR}$ (400 MHz, CDCl_3) δ 14.2, 22.7, 29.3, 32.7, 52.3, 121.4, 122.8, 123.4, 124.2, 124.4, 127.0, 127.2, 127.3, 129.9, 130.0, 132.0, 170.5. FT-IR: 2956 cm^{-1} (w), 2927 (w), 2859 (w), 1754 (w), 1694 (s), 1393 (w), 1357 (m), 1309 (w), 830 (s). HRMS (ESI): $m/z = 471.22$ (M^+) Anal.: $\text{C}_{33}\text{H}_{29}\text{NO}_2$ Calcd., C (84.05), H (6.20), N (2.97), O (6.97); Found, C (83.88), H (6.19), N (3.07), O (6.86).

2-(Undecan-6-yl)-1H-perylene[1,12-efg]isoindole-1,3(2H)-dione (3c). A 1.45-g portion, 4.19 mmol, of (1) was added to a solution of (2c) (1.50 g, 8.81 mmol) in DMA (100 mL) and refluxed overnight. The solution was cooled to room temperature, and methanol (230 mL) was added to complete crystallization of the imide. The obtained solid was dissolved in hot 5:6 toluene/hexane and purified by column chromatography (silica, toluene/hexane, $R_f = 0.60$), and finally boiled out in 1:1 methanol/water (200 mL), leaving (3c) as a yellow powder (1.81 g, 86%). Mp.: $221\text{--}223^\circ\text{C}$ $^1\text{H NMR}$ (400 MHz, CDCl_3): δ 9.17 (d, $J = 8.7\text{ Hz}$, 2H), 8.90 (d, 7.8 Hz, 2H), 8.15 (d, 8.2 Hz, 2H), 8.12 (d, 9.2 Hz, 2H), 8.02 (t, 7.8 Hz, 2H), 4.40 (sept, 5.0 Hz, 1H), 2.21–2.33 (m, 2H), 1.82–1.93 (m, 2H), 1.25–1.48 (m, 12H), 0.86 (t, 7.3 Hz, 6H) $^{13}\text{C NMR}$ (400 MHz, CDCl_3) δ 14.2, 22.7, 26.8, 31.8, 32.9, 52.3, 121.3, 122.7, 123.3, 124.1, 124.2, 126.8, 127.1, 127.2, 129.7, 129.9, 131.9, 170.5. FT-IR: 2956 cm^{-1} (w), 2927 (w), 2859 (w), 1754 (w), 1694 (s), 1393 (w), 1357 (m), 1309 (w), 830 (s). HRMS (ESI): $m/z = 499.25$ (M^+) Anal.: $\text{C}_{35}\text{H}_{33}\text{NO}_2$ Calcd., C (84.14), H (6.66), N (2.80), O (6.40); Found, C (84.11), H (6.66), N (2.79), O (6.44).

2-(Tridecan-7-yl)-1H-perylene[1,12-efg]isoindole-1,3(2H)-dione (3d). A 1.2416-g portion of (1) (3.59 mmol) was dissolved in 75 mL DMA in a 250-mL two-neck, round-bottom equipped with stir bar and condenser. The solution was brought to 125°C with stirring to which 1.5643 g (2d) (7.86 mmol) was added. The reaction was allowed to stir overnight and an orange precipitate formed upon cooling back to room temperature. A 50-mL portion of CHCl_3 was added and 1.5883 g crude product collected. Crude (3d) was washed with 2 M HCl, followed by 75:25 MeOH/ H_2O , and then boiled in hot hexane for 2 h before filtering hot. Recrystallization from hexane yielded 1.4370 g (3d) as a bright orange powder. (76%) Mp.: $186\text{--}188^\circ\text{C}$ $^1\text{H NMR}$ (400 MHz, CDCl_3): δ 9.30 (d, $J = 7.5\text{ Hz}$, 2H), 9.09 (d, 7.4 Hz, 2H), 8.25 (d, 6.8 Hz, 2H), 8.20 (d, 8.7 Hz, 2H), 8.12 (t, 5.0 Hz, 2H), 4.40 (sept, 1H), 2.20–2.30 (q, 2H), 1.80–1.90 (q, 2H), 1.20–1.45 (m, 16H), 0.82 (t, 6.9 Hz, 6H). $^{13}\text{C NMR}$ (400 MHz, CDCl_3) δ 14.2, 22.7, 27.1, 29.3, 31.9, 33.0, 52.4, 121.4, 122.8, 123.4, 124.2, 124.4, 127.0, 127.3, 127.4, 129.9, 130.0, 132.0, 170.5. FT-IR: 2956 cm^{-1} (w), 2927 (w), 2859 (w), 1754 (w), 1694 (s), 1393 (w), 1357 (m), 1309 (w), 830 (s). HRMS (ESI): $m/z = 528.29$ ($\text{M}+1$) $^+$ Anal.: $\text{C}_{37}\text{H}_{37}\text{NO}_2$ Calcd., C

(84.22), H (7.07), N (2.65), O (6.06). Found, C (83.85), H (7.09), N (2.73), O (6.33).

■ ASSOCIATED CONTENT

Supporting Information. Compound characterization data and detailed instrumental methods. This material is available free of charge via the Internet at <http://pubs.acs.org>.

■ AUTHOR INFORMATION

Corresponding Author

*E-mail: lkelly@umbc.edu.

■ REFERENCES

- (1) Avlasevich, Y.; Chen, L.; Mullen, K. *J. Mater. Chem.* **2010**, *20*, 3814–3826.
- (2) Herrmann, A.; Mullen, K. *Chem. Lett.* **2006**, *35*, 978–985.
- (3) Langhals, H. *Heterocycles* **1995**, *40*, 477–500.
- (4) Ebeid, E.; El-Daly, S. A.; Langhals, H. *J. Phys. Chem.* **1988**, *92*, 4565–4568.
- (5) Rademacher, A.; Maerke, S.; Langhals, H. *Chem. Ber.* **1982**, *115*, 2927–2934.
- (6) Demmig, S.; Langhals, H. *Chem. Ber.* **1988**, *121*, 225–230.
- (7) Peneva, K.; Gundlach, K.; Herrmann, A.; Paulsen, H.; Mullen, K. *Org. Biomol. Chem.* **2010**, *8*, 4823–4826.
- (8) Tomizaki, K.; Loewe, R. S.; Kirmaier, C.; Schwartz, J. K.; Retsek, J. L.; Bocian, D. F.; Holten, D.; Lindsey, J. S. *J. Org. Chem.* **2002**, *67*, 6519–6534.
- (9) Diaz-Garcia, M. A.; Calzado, E. M.; Villalvilla, J. M.; Boj, P. G.; Quintana, J. A.; Cespedes-Guirao, F. J.; Fernandez-Lazaro, F.; Sastre-Santos, A. *Synth. Met.* **2009**, *159*, 2293–2295.
- (10) Nijegorodov, N.; Mabbs, R.; Downey, W. S. *Spectrochim. Acta, A* **2001**, *57A*, 2673–2685.
- (11) Gvishi, R.; Reisfeld, R.; Burshtein, Z. *Chem. Phys. Lett.* **1993**, *213*, 338–344.
- (12) Lohmannsroben, H. G.; Langhals, H. *Appl. Phys. B: Laser Opt.* **1989**, *48*, 449–452.
- (13) Sadrai, M.; Bird, G. R. *Opt. Commun.* **1983**, *51*, 62–64.
- (14) Sadrai, M.; Hadel, L.; Sauers, R. R.; Husain, S.; Krogh-Jepersen, K.; Westbrook, J. D.; Bird, G. R. *J. Phys. Chem.* **1992**, *96*, 7988–7996.
- (15) Rao, K.; George, S. J. *Org. Lett.* **2010**, *12*, 2656–2659.
- (16) Zhang, X.; Chen, Z.; Wurthner, F. *J. Am. Chem. Soc.* **2007**, *129*, 4886–4887.
- (17) Che, Y.; Datar, A.; Balakrishnan, K.; Zang, L. *J. Am. Chem. Soc.* **2007**, *129*, 7234–7235.
- (18) Langhals, H. *Helv. Chim. Acta* **2005**, *88*, 1309–1343.
- (19) Balakrishnan, K.; Datar, A.; Oitker, R.; Chen, H.; Zuo, J.; Zang, L. *J. Am. Chem. Soc.* **2005**, *127*, 10496–10497.
- (20) Qu, J.; Zhang, J.; Grimsdale, A. C.; Mullen, K.; Jaiser, F.; Yang, X.; Neher, D. *Macromolecules* **2004**, *37*, 8297–8306.
- (21) Wurthner, F. *Chem. Commun.* **2004**, *14*, 1564–1579.
- (22) Langhals, H.; Speckbacher, M. *Eur. J. Org. Chem.* **2001**, *13*, 2481–2485.
- (23) Alibert-Fouet, S.; Seguy, I.; Bobo, J.; Destuel, P.; Bock, H. *Chem.—Eur. J.* **2007**, *13*, 1746–1753.
- (24) Barentsen, H. M.; van Dijk, M.; Kimkes, P.; Zuilhof, H.; Sudholter, E. J. R. *Macromolecules* **1999**, *32*, 1753–1762.
- (25) Langhals, H.; Grudner, S. *Chem. Ber.* **1986**, *119*, 2373–2376.
- (26) Langhals, H.; Ismael, R.; Yuruk, O. *Tetrahedron* **2000**, *56*, 5435–5441.
- (27) Langhals, H.; Demmig, S.; Huber, H. *Spectrochim. Acta, A* **1988**, *44A*, 1189–1193.
- (28) Reichardt, C. *Chem. Rev.* **1994**, *94*, 2319–2358.
- (29) Clar, E.; Zander, M. *J. Chem. Soc.* **1957**, *65*, 4616–4619.
- (30) Clar, E.; Frommel, H. *Chem. Ber.* **1949**, *82*, 46–60.
- (31) Clar, E. *Chem. Ber.* **1932**, *65B*, 846–858.
- (32) Borch, R. F.; Bernstein, M. D.; Durst, H. D. *J. Am. Chem. Soc.* **1971**, *93*, 2897–2904.
- (33) Langhals, H.; Jona, W. *J. Org. Chem.* **1998**, 847–851.
- (34) Langhals, H.; Poxleitner, S.; Krotz, O.; Pust, T.; Walter, A. *Eur. J. Org. Chem.* **2008**, 4559–4562.
- (35) Zoon, P. D.; Brouwer, A. *ChemPhysChem* **2005**, *6*, 1574–1580.
- (36) Kajiwara, T.; Shirotani, I.; Inokuchi, H.; Iwashima, S. *J. Mol. Spectrosc.* **1969**, *29*, 454–460.
- (37) Turro, N. J.; Ramamurthy, V.; Scaiano, J. C. In *Principles of Molecular Photochemistry*; University Science Books: Sausalito, CA, 2009.
- (38) Langhals, H.; Demmig, S.; Potrawa, T. *J. Prakt. Chem.* **1991**, *333*, 733–748.
- (39) Mataga, N.; Kaifu, Y.; Koizumi, M. *Bull. Chem. Soc. Jpn.* **1956**, *29*, 465–470.
- (40) Kasha, M. *Faraday Discuss.* **1950**, *9*, 14–19.
- (41) Birks, J. B. *Chem. Phys. Lett.* **1972**, *17*, 370–372.
- (42) Beer, M.; Longuet-Higgins, H. C. *J. Chem. Phys.* **1955**, *23*, 1390–1391.
- (43) Brokkehurst, B.; Young, R. N. *J. Phys. Chem. A* **1999**, *103*, 3818–3824.
- (44) Schael, F.; Lohmannsriebe, H. G. *J. Photochem. Photobiol. A* **1992**, *69*, 27–32.
- (45) Birks, J. B.; Easterly, C. E.; Christophorou, L. G. *J. Chem. Phys.* **1977**, *66*, 4231–4236.
- (46) Carter, J. G.; Christophorou, L. G.; Easterly, C. E. *J. Chem. Soc., Faraday Trans. II* **1973**, *69*, 471–483.
- (47) Dawson, W. R.; Kropp, J. L. *J. Chem. Phys.* **1968**, *73*, 1752–1758.